

**Electronic coarse graining enhances the predictive power of molecular simulation allowing challenges in water physics to be addressed**  
by Flaviu S. Cipcigan, Vlad P. Sokhan, Jason Crain and Glenn J. Martyna

Preprint accepted in the Journal of Computational Physics.  
[dx.doi.org/10.1016/j.jcp.2016.08.030](https://doi.org/10.1016/j.jcp.2016.08.030)

# Electronic coarse graining enhances the predictive power of molecular simulation allowing challenges in water physics to be addressed

Flaviu S. Cipcigan<sup>a,b</sup>, Vlad P. Sokhan<sup>b</sup>, Jason Crain<sup>a,b</sup>, Glenn J. Martyna<sup>c</sup>

<sup>a</sup>*School of Physics and Astronomy, University of Edinburgh, Peter Guthrie Tait Road, Edinburgh EH9 3FD, United Kingdom*

<sup>b</sup>*National Physical Laboratory, Hampton Road, Teddington, Middlesex TW11 0LW, United Kingdom*

<sup>c</sup>*IBM T. J. Watson Research Center, Yorktown Heights, New York 10598, USA*

---

## Abstract

One key factor that limits the predictive power of molecular dynamics simulations is the accuracy and transferability of the input force field. Force fields are challenged by heterogeneous environments, where electronic responses give rise to biologically important forces such as many-body polarisation and dispersion. The importance of polarisation was recognised early-on and described by Cochran in 1959 [1, 2]. However, dispersion forces are still treated at the two-body level and in the dipole limit, although the importance of three-body terms in the condensed phase was demonstrated by Barker in the 1980s [3, 4]. A way of treating both polarisation and dispersion on an equal basis is to coarse grain the electrons a molecular moiety to a single quantum harmonic oscillator, as suggested as early as the 1960s by Hirschfelder, Curtiss and Bird [5]. This treatment, when solved in the strong coupling limit, gives all orders of long-range forces. In the last decade, the tools necessary to exploit this strong coupling limit have been developed, culminating in a transferable model of water with excellent predictive power across the phase diagram. This transferability arises since the environment identifies the form of long range interactions, rather than the expressions selected by the modeller. Here, we discuss the role of electronic coarse-graining in predictive multiscale materials modelling and describe the first implementation of the method in a general purpose molecular dynamics software, QDO.MD.

*Keywords:* molecular dynamics, force field, electronic coarse graining, dispersion, polarisation, path integral

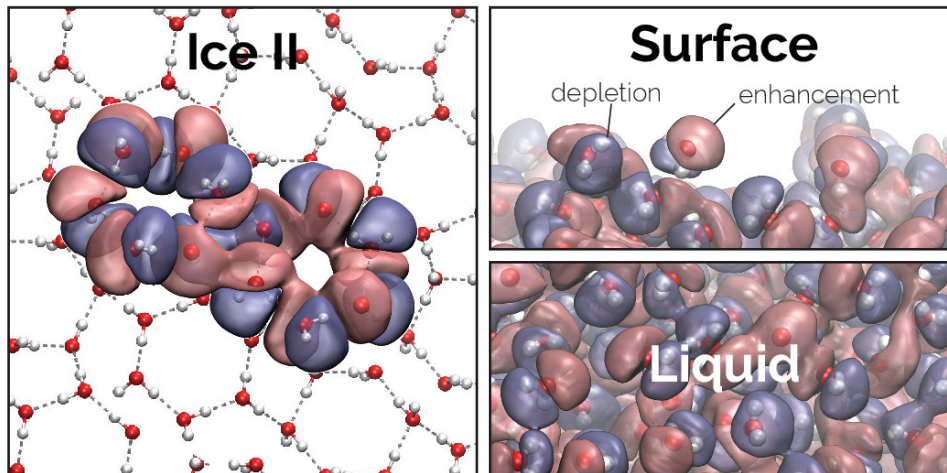


Figure 1: Examples of environments where the properties of QDO-water have been studied and shown to match experiment: ice II, ambient temperature liquid and the surface of the liquid. The images illustrate the electronic responses of individual molecules, with red and blue isosurfaces corresponding to regions of enhancement and depletion of electronic density, respectively.

---

## 1. Introduction

Molecular modelling has become an integral part of research in all areas of condensed matter, forming a new part of the scientific method that elucidates principles and accelerates the discovery of new materials [6, 7]. This computational revolution has been driven by the exponential scaling of computer hardware [8, 9] along with the implementation of scalable software on these platforms [10, 11, 12, 13]. An important part of the equation remains to improve the accuracy and transferability of the employed force fields, which ultimately define the accuracy of results and lay the basis for predictive modelling, given sufficient sampling of phase space.

Standard force fields, designed to be numerically efficient, are created by fitting a subset of thermodynamic and structural properties to an analytic expression for the potential energy, typically consisting of sums of pairwise terms [14]. In many systems, this approach has proved successful even if the accuracy of such force fields is as best around 1 kcal/mol. For example,

Schames et al. [6] used molecular dynamics simulations to discover a hidden binding site in HIV integrase, a molecule that enables the integration of HIV’s genetic material into the host cell DNA. This discovery led to experimental confirmation [15] and subsequent development of raltegravir, a successful medicine that halts the progression of HIV into AIDS. Another success was the simultaneous discovery by simulation [16] and experiment [17] of the molecular basis of mutations in a gene responsible for Gaucher’s disease, a genetic disease causing the build-up of fatty substances in the organism.

Nonetheless, strategies based on fitting to a fixed functional are not guaranteed to be transferable to heterogeneous environments far from the region of parametrisation. One such environment is, for example, a bacterial membrane penetrated by a peptide. The shape of the peptide inside the membrane depends strongly on the force fields used [18], with only experiments currently being able to distinguish between possibilities.

Here we present our recent development of a force field for materials modelling [19, 20, 21, 22, 23, 24, 25] that is transferable, physically motivated, and implemented in the general purpose molecular dynamics software QDO\_MD. The technique treats many-body polarisation and many-body dispersion on the same footing by representing electronic distributions of individual atoms and molecular moieties using a single coarse grained particle. This particle, known as a Quantum Drude Oscillator [24, 25] (QDO), consists of a negative charge bound to a positive centre by a quantum harmonic oscillator. QDOs generate many-body polarization, many-body dispersion interactions and cross terms beyond the dipole limit [26] and represent a non-perturbative approach that generates all long-range forces within Gaussian statistics when sampled in strong coupling.

The QDO approach has been employed to construct a general purpose water model (QDO-water) that is transferable without fitting to any condensed phase data (neglecting bond breaking and making). QDO-water consists of a rigid molecular geometry (made out of fixed charges), short-range empirical repulsion and a QDO. The model is parametrised using the static multiple moments of an isolated molecule, its polarisability, the dipole-dipole dispersion coefficient ( $C_6$ ) and the energy landscape of the dimer. Its properties have been studied in a diverse set of environments (depicted in Fig. 1), ranging from high-pressure ice (ice II), liquid water, steam, the liquid-vapour interface, and supercritical water. The model predicts density, surface tension, enthalpy of vaporisation and dielectric constant across these wide range of environments, demonstrating a formerly unrealized level of transferability.

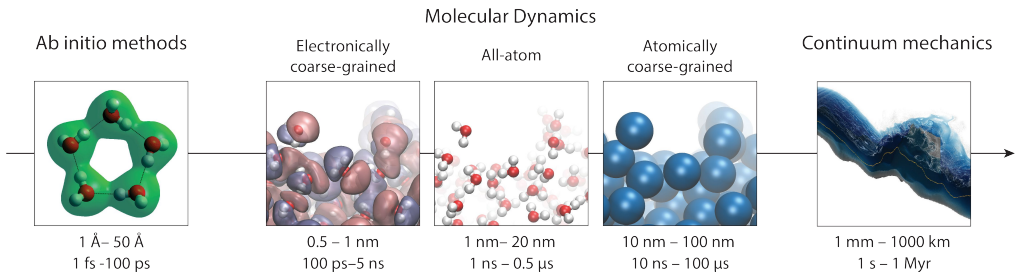


Figure 2: Various simulation techniques arranged according to the timescales and length-scales which they sample. The left-most image, originally by Chaplin [27], represents electron densities of the water pentamer obtained via ab initio calculations. The next is the electronically coarse grained representation of the air-water surface, where red and blue isosurfaces depict regions of enhancement and depletion of electronic density. This is followed by a classical molecular dynamics simulation and an atomically coarse grained study of the same interface. The right-most image represents a particle-based realtime simulation of water flow over complex landscape using a method developed by Chentanez and Müller [28]. The left and right-most images are used with permission from their respective authors while the rest are original work by the authors of this paper.

## 2. Predictive materials modelling using electronically coarse grained methods

Fig. 2 shows where the QDO method stands on the spectrum of modelling techniques, occupying a previously vacant place between ab initio methods and all-atom molecular dynamics. QDOs’ guiding philosophy is “instead of treating an exact system in an approximate way, treat an approximate system in an exact way”.

In a physical sense, the QDO model is solvable in strong coupling, allowing for an approach that contains all long-range, many-body interactions to all orders. The lack of truncation means that the modeller does not pick the symmetry by choice of truncation but rather the environment picks the key terms. This type of simplified but rich model is at the heart of modern theories because its lack of bias allows the essential physics to emerge naturally.

The price paid for the richness of the QDO model at low computational cost (order  $N$ ) is the approximation made in coarse graining: assuming localized electrons in an insulator respond according to Gaussian statistics and the neglect of exchange effects, which are assumed to be short range. This

is consistent with the general spirit of coarse grained approaches where exactness is sacrificed while maintaining sufficient accuracy for the problem at hand. Basically, QDOs are a coarse graining of a full high level electronic structure due to their lack of truncation, while standard force fields are a coarse graining of QDOs, with a truncation to dipole limit pair-wise dispersion and a neglect of polarization or its inclusion at the many-body dipole level. As demonstrated in the next section, systems of single QDOs per atom or molecular moiety solved in strong coupling are sufficient to model molecules that are isotropic (such as noble gases) or close to isotropic (such as simple hydrides like methane and water). To model anisotropic responses, multiple QDOs can be pinned to individual points in the molecular frame [29].

Water is an ideal system in which to illustrate the importance of a complete treatment of electronic responses. Water’s structure arises due to a competition between directional hydrogen bonds, which favour an open ice-like local structure and van der Waals forces, which favour a close-packed local structure. Many-body polarization and dispersion interaction are key to distinguishing the dominant motifs *under the conditions of interest*.

Hydrogen bonds are known to be cooperative, meaning that their interaction strength changes depending on environment thus leading to a wide variety of motifs emerging. A simple reporter of this cooperation is the molecular dipole moment, which changes from a value of 1.85 D in the gas phase to an estimated value of 2.5–3.6 D in liquid [23, 30], where four hydrogen bonded motifs are dominant. This sensitivity to local structure can be used as a fingerprint of various local motifs, as we have reported in reference [20]. There, we showed that a cusp in the dipole moment as a function of temperature coincides with experimental maxima in heat capacity, separating the supercritical region in “gas-like” and “liquid-like” regions [31] and revealing the liquid-gas Widom line [32] at a molecular level. We also showed that such cooperation makes hydrogen bonds more asymmetric than previously thought [21], with a molecule favouring the loss of an acceptor bond (on the side of the oxygen) over that of a donor bond (on the side of the hydrogen) in both the liquid phase and at the liquid–gas interface.

Dispersion interactions are also important in water. Including these responses is essential to generate even the basic structure of water at room temperature. An illustrative example of this balance is the overstructuring of room-temperature water by DFT [33], where including the electron correlations that lead to accurate van der Waals interactions is challenging

(although, there have been promising results using a similar technique of embedded quantum harmonic oscillators at the dipole level [34]). In our water model the dispersion coefficients are tunable, while keeping the polarisation fixed, by changing the parameters of the QDO. In Ref. [23], we showed that by changing the strength of van der Waals interactions, the density of liquid water can be changed by 15% while still keeping a hydrogen bonded local structure.

In addition, three-body effects account for as much as 25% of the binding energy of water, according to the estimates of Keutsch et al. [35]. Thus, monoatomic two-body potentials for the water molecule can only reproduce water’s condensed phase properties if their parameters are allowed to vary with state point [36, 37]. Even a full-atom description of water cannot be transferable if its electrostatics is fixed. Vega and Abascal [38] showed that a nonpolarisable model of water cannot simultaneously be fit to the melting temperature and temperature of maximum density.

Therefore, in order to create a truly transferable energy surface for molecular simulations, which is therefore predictive outside the regime of parametrisation, the electronic effects need to be taken into account since they give rise to non-trivial many-body polarization and dispersion. QDOs do so while keeping efficiency close to that of all-atom molecular dynamics and scaling as  $N \log N$  with the number of atoms  $N$ . This strategy can be used to create models that are parametrised without any condensed phase input, yet generate the properties of condensed phases.

### 3. Electronic coarse graining using Quantum Drude Oscillators

#### 3.1. Dispersion interactions between quantum harmonic oscillators

In order to gain intuition into how quantum harmonic oscillators replicate electronic responses, consider a simple model [39]: a negative charge  $-q$  of mass  $m$ , free to move in a dimension  $x$ . The charge is localised by connecting it by a spring of frequency  $\omega$  to a positive charge  $+q$  fixed at the origin.

Consider adding a positive, fixed test charge  $Q$  at a distance  $R \gg x$  from the origin. The system is in equilibrium when the Coulomb force  $Eq$  on the negative charge equals the spring force  $m\omega^2x$ . Balancing the two forces results in the oscillator acquiring a dipole moment  $\mu = qx = \frac{q^2E}{m\omega^2}$  and thus having a dipole polarisability defined as:

$$\alpha_1 := \frac{\mu}{E} = \frac{q^2}{m\omega^2}. \quad (1)$$

In order to account for dispersion effects, the system has to be treated quantum mechanically. Consider two identical oscillators separated by a distance  $R$  interacting via a term  $c(R)$ . The leading order interaction is dipole-dipole, meaning that the term  $c(R)$  is proportional to  $R^{-3}$ . Thus, the Hamiltonian is:

$$\hat{H} = \frac{\hat{p}_1^2}{2m} + \frac{\hat{p}_2^2}{2m} + \frac{1}{2}m\omega^2 (x_1^2 + x_2^2 + c(R)x_1x_2) . \quad (2)$$

Changing coordinates to  $\hat{\rho}_{\pm} = \frac{1}{\sqrt{2}}(\hat{p}_1 \pm \hat{p}_2)$  and  $\xi_{\pm} = \frac{1}{\sqrt{2}}(x_1 \pm x_2)$  decouples the Hamiltonian into two independent harmonic oscillators of frequency  $\omega\sqrt{1 \pm c}$ .

$$\hat{H} = \left( \frac{\hat{p}_+^2}{2m} + \frac{1}{2}m\omega^2 (1 + c) \xi_+^2 \right) + \left( \frac{\hat{p}_-^2}{2m} + \frac{1}{2}m\omega^2 (1 - c) \xi_-^2 \right) \quad (3)$$

The ground state energy of the coupled system is hence given by, to leading order in  $c$ :

$$E_0 = \frac{1}{2}\hbar\omega \left( \sqrt{1 + c} + \sqrt{1 - c} \right) \\ \approx \hbar\omega \left( 1 - \frac{1}{8}c^2 + O(c^3) \right) . \quad (4)$$

Fig. 3 shows the ground state probability distribution  $\psi^2(x_1, x_2)$  in the independent ( $c = 0$ ) and correlated ( $c > 0$ ) cases. When  $c$  increases, it becomes more probable for  $x_1$  and  $x_2$  to have the opposite sign and less probable for them to have the same sign. Since the energy is proportional to  $\int dx_1 dx_2 \psi^2(x_1, x_2)x_1x_2c(R)$ , this correlation leads to the attractive force between two neutral molecules proportional to  $-c(R)^2 \sim -R^{-6}$ , just as the leading order term in the van der Waals potential.

This analysis shows that a one dimensional quantum harmonic oscillator can capture two basic effects of long range forces: polarisation and dispersion. In this case, these interactions are limited to dipole-limit forces. To capture the full set of interactions one has to consider the full three dimensional system.

### 3.2. Full quantum model

A Quantum Drude Oscillator (QDO) [24] is made out of a light, negative particle of charge  $q$  connected to a heavy positive *centre* by a harmonic spring

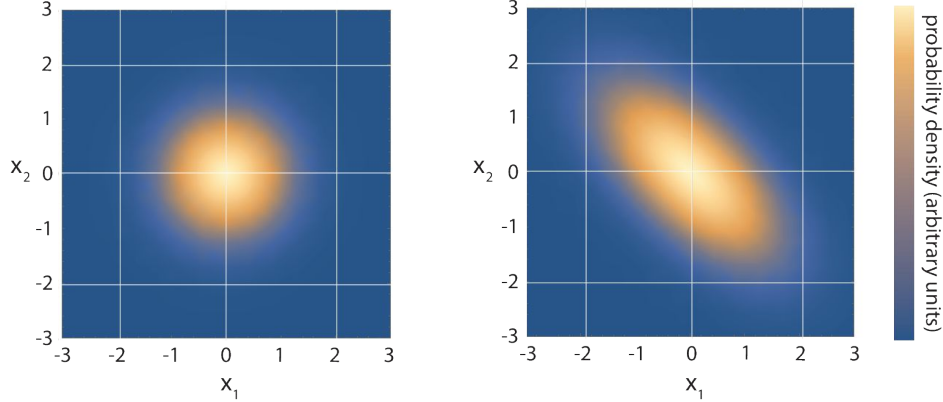


Figure 3: The ground state probability density of two one dimensional quantum harmonic oscillators interacting via a  $c(R)x_1x_2$  term. The left panel illustrates the non-interacting case, with  $c(R) = 0$ . The right panel illustrates the interacting case, with  $c(R) > 0$ . The spread of the wavefunction across the diagonal represents the electron correlation that gives rise to attractive van der Waals forces in real systems.

of frequency  $\omega$ . The bound state of this system is a *drudon*, with reduced mass  $m$  and Hamiltonian

$$\hat{H} = \frac{\hat{\mathbf{p}}^2}{2m} + \frac{1}{2}m\omega^2\mathbf{x}^2. \quad (5)$$

Perturbing this Hamiltonian via a point charge  $Q$  at a distance  $R$  gives a first order correction to the energy of zero and a second order correction of [26]:

$$E^{(2)} = - \sum_{l=0}^{\infty} \frac{Q^2\alpha_l}{2R^{2l+2}}, \quad (6)$$

where the polarisabilities  $\alpha_l$  are given by

$$\alpha_l = \left[ \frac{q^2}{m\omega^2} \right] \left[ \frac{(2l-1)!!}{l} \right] \left[ \frac{\hbar}{2m\omega} \right]^{l-1}. \quad (7)$$

Considering two QDOs separated by a distance  $R$  gives a first order correction to the energy of zero and a second order correction of [26, 40]:

$$E^{(2)} = - \sum_{n=3}^{\infty} C_{2n}R^{-2n} \quad (8)$$

with

$$\begin{aligned}
 C_6 &= \frac{3}{4}\alpha_1\alpha_1\hbar\omega, \\
 C_8 &= 5\alpha_1\alpha_2\hbar\omega, \\
 &\dots
 \end{aligned}
 \tag{9}$$

Therefore, the full model has a complex and rich set of long range responses, which are replicated with only three parameters. This means the responses are correlated and thus one needs to check whether these correlations are satisfied in real atoms and molecules.

### 3.3. Invariant relationships between response coefficients

As the responses of QDOs depend only on three parameters, these parameters can be eliminated, resulting in the following invariants that can be used to verify the accuracy of the QDO approximation [26]:

$$\begin{aligned}
 \sqrt{\frac{20}{9}} \frac{\alpha_2}{\sqrt{\alpha_1\alpha_3}} &= 1, \\
 \sqrt{\frac{49}{40}} \frac{C_8}{\sqrt{C_6C_{10}}} &= 1, \\
 \frac{C_6\alpha_1}{4C_9} &= 1.
 \end{aligned}
 \tag{10}$$

Comparing these ratios with the responses of real molecules gives the results shown in Fig. 4 (reproduced from Ref. [26]).

The agreement is good for the noble gases, with ratios within 10% of experiment, as their shells are fully filled and thus the distribution of electrons is nearly spherical. The agreement is also within 10% for most alkali metals, for which the last electron contributes mostly to polarisation. Small hydrides such as water and methane agree within 15%. This agreement is due to the electronegativity of atoms such as oxygen, which centres most of the electronic charge on them thus resulting in charge distributions and responses that are close to spherical.

### 3.4. Parametrisation

Aside invariants, the responses of a QDO can be inverted to give its properties as a function of the responses. The relevant relations, which are used to parametrise a QDO are as follows:

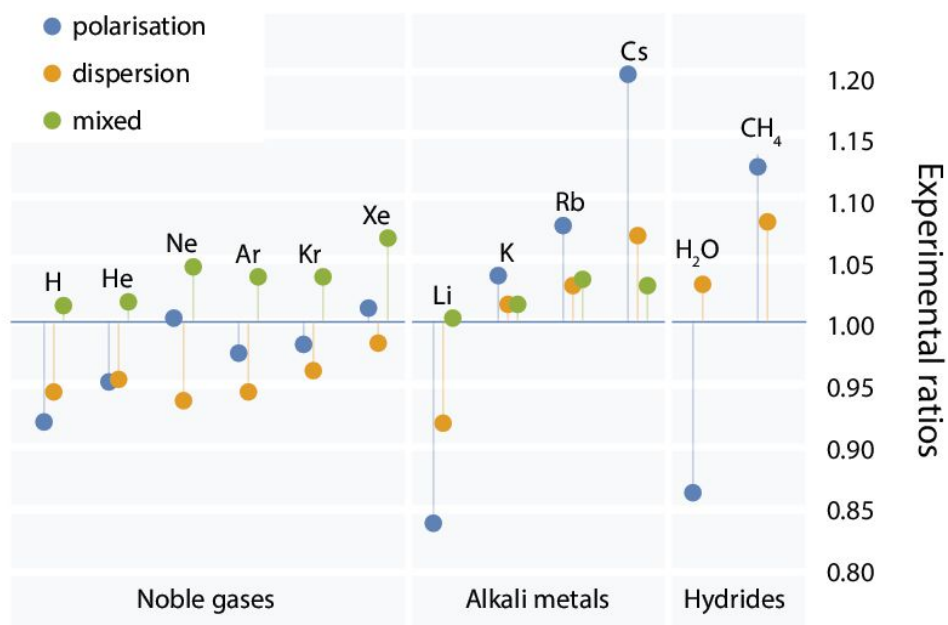


Figure 4: Three types of invariant ratios between polarisation and dispersion coefficients, predicted by Quantum Drude Oscillators. Polarisation ratios involve only polarisation coefficients and analogously for dispersion ratios. Mixed ratios involve both polarisation and dispersion coefficients. Deviation from theory is shown for three types of atoms and molecules: noble gases, alkali metals and small hydrides.

$$\omega = \frac{1}{\hbar} \frac{4C_6}{3\alpha_1^2}, \quad (11)$$

$$m = \frac{\hbar}{\omega} \frac{3\alpha_1}{4\alpha_2} \quad \text{or} \quad m = \frac{\hbar}{\omega} \frac{5C_6}{C_8}, \quad (12)$$

$$q = -\sqrt{m\omega^2\alpha_1}. \quad (13)$$

#### 4. Simulating Quantum Drude Oscillators via two temperature path integral molecular dynamics

Path integral molecular dynamics, shortened to PIMD, is a method of sampling a quantum mechanical partition function such as that of a QDO, using classical methods [41, 42]. This section highlights its basic derivation, with the full, QDO-based method being described in Refs. [25, 22].

Consider a quantum mechanical system with degrees of freedom  $\vec{x}$  whose state is described by a density matrix  $\rho(\vec{x}, \vec{x}')$ . The partition function of the system is [43]:

$$Z(\beta) = e^{-\beta\hat{H}} = \int \mathbf{d}\vec{x} \rho(\vec{x}, \vec{x}; \beta), \quad (14)$$

where  $\mathbf{d}\vec{x}$  represents a small volume element in the  $\dim(\vec{x})$ -dimensional space spanned by the system's degrees of freedom.

Since the density matrix is an exponential, it can be factorised into higher temperature (smaller  $\beta$ ) slices to give the following path integral representation,

$$Z(\beta) = \prod_{i=1}^P \int \mathbf{d}\vec{x}_i \rho(\vec{x}_i, \vec{x}_{i+1}; \beta/P). \quad (15)$$

The reason for this factorisation is the fact that increasing the temperature, thus decreasing  $\beta$  makes density matrices more classical and thus easier to approximate. The approximation used comes from a Trotter factorisation [25, 44], where the Hamiltonian is split into a reference  $\hat{H}_0$ , with known density matrix  $\rho_0 = e^{-\tau\hat{H}_0}$  and a perturbation  $V(\vec{x})$  as follows:

$$\rho(\vec{x}, \vec{x}'; \tau) \approx e^{-\tau V(\vec{x})/2} \rho_0(\vec{x}, \vec{x}'; \tau) e^{-\tau V(\vec{x}')/2} + O(\tau^3). \quad (16)$$

In the case of QDOs,  $H_0$  is the Hamiltonian of the isolated system, with the following reference density matrix:

$$\rho_0(\vec{x}_i, \vec{x}_{i+1}; \tau) = \left[ \frac{\alpha_P(\tau)}{\pi} \right] \exp \left[ \alpha_P(\tau)(\vec{x} - \vec{x}')^2 + \frac{\lambda_P(\tau)}{2}(\vec{x}^2 + (\vec{x}')^2) \right]. \quad (17)$$

The coefficients  $\alpha_P(\tau)$  and  $\lambda_P(\tau)$  are defined in Appendix A.

Note that this form introduces strong nearest-neighbour coupling between the coordinates  $\vec{x}_i$ . To remove this coupling, the density matrix is diagonalised to the independent coordinates  $\vec{u}_i$  via a staging transformation with unit Jacobian [25]. The coefficients of the transformation are given in Appendix A, leading to the following partition function:

$$\begin{aligned}
Z(\beta) &= \prod_{i=1}^P \int \mathbf{d}\vec{x}_i \rho_0(\vec{x}_i, \vec{x}_{i+1}; \tau) \times \exp\left(-\tau \sum_{i=1}^P V(\vec{x}_i)\right) \\
&= \prod_{i=1}^P \int \mathbf{d}\vec{u}_i \underbrace{\left(\frac{1}{2\pi\sigma_i^2}\right)^{3N/2} \exp\left(-\frac{\vec{u}_i^2}{2\sigma_i^2}\right)}_{\text{staging coordinates}} \times \underbrace{\exp\left(-\tau \sum_{i=1}^P V(\vec{x}_i(\vec{u}_i))\right)}_{\text{external potential}}.
\end{aligned} \tag{18}$$

One step remains in order to make the partition function isomorphic to the classical limit: the addition of conjugate momenta  $\vec{p}_i$  with corresponding faux masses  $m_i$ . This transforms it to

$$\begin{aligned}
Z(\beta) &= \prod_{i=1}^P \int \mathbf{d}\vec{u}_i \left(\frac{1}{2\pi\sigma_i^2}\right)^{3N/2} \exp\left(-\frac{\vec{u}_i^2}{2\sigma_i^2}\right) \times \exp\left(-\tau \sum_{i=1}^P V(\vec{x}_i(\vec{u}_i))\right) \\
&\quad \times C \int \mathbf{d}\vec{p}_i \exp\left(-\tau \frac{\vec{p}_i^2}{2m_i}\right).
\end{aligned} \tag{19}$$

This final transformation leads to a partition function with the effective classical Hamiltonian  $H^{(\text{faux})}$ , which can be sampled via existing classical means [42, 24, 25]

$$H^{(\text{faux})} = \sum_{i=1}^P \frac{\vec{p}_i^2}{2m_i} + \frac{\vec{u}_i^2}{2\sigma_i^2\tau} + \frac{V(\vec{x}_i(\vec{u}_i))}{P}. \tag{20}$$

When adding nuclei, the adiabatic principle needs to be invoked and the temperature of the electronic degrees of freedom increased by a factor of  $\gamma$  relative to that of the nuclear degrees of freedom to reduce the number of beads required for convergence. [42, 24, 25, 22]

## 5. QDO\_MD: a molecular dynamics software implementing Quantum Drude Oscillators

The QDO methodology has been implemented in QDO\_MD, a new software based on the work of the Tuckerman and Martyna groups that includes a classical molecular dynamics engine, Car–Parrinello ab initio molecular dynamics (CPAPIMD) [45] using plane wave basis set, as well as a QM/MM capability with  $N \log(N)$  scaling. QDO\_MD encompasses a number of advanced algorithms including parallel tempering [46] and centroid path integral propagators for nuclear degrees of freedom [11]. The force field based part of the software has the standard force fields built in, targeting complex chemical and biological applications. QDO\_MD is based on a number of algorithms developed by its principal authors, which are now widely accepted, including reversible reference system propagator (RESPA) [47], Nosé–Hoover chains [48] and isothermal–isobaric ensemble [49] and allows simulation in various equilibrium statistical ensembles, perform energy and structure minimization using several techniques including steepest descent, conjugate gradient or direct inversion in the iterative subspace. It is parallelised [50] at several levels including classical force parallelisation, parallelisation over beads in path integral simulation, state and hybrid state/reciprocal space parallelisation of the electrostatic interactions and is aimed at distributed memory architectures using the Message Passing Interface (MPI) protocol [51]. QDO\_MD is undergoing an extensive refactoring and is currently available by contacting the authors. In the near future, it will be placed on the National Physical Laboratory website and open sourced on GitHub.

QDO\_MD has modular structure and easily allows extensions conforming to the accepted structure. In order to perform adiabatic path integral molecular dynamics with QDO (APIMD-QDO), a new simulation type keyword, `qdo_pimd`, has been added. Two new atom types, `drude_bead` and `drude_center` specify the drudon. For generality, the Drude oscillator centres are treated as ghost atoms. Electrostatic interactions in QDO\_MD are calculated using smooth particle mesh Ewald (PME) method [52], and in addition to standard 3D-periodic systems the code can handle the systems of reduced dimensionality using modified reciprocal space summation [53, 54]. Although drudons do not introduce new types of interactions, special terms have been added between the bead and the centre in drudon to correct for terms necessary included in the reciprocal space part of the Ewald scheme. In addition to that, Coulomb regularisation has been added at short range

as well as triexponential repulsion terms to correct for the missing exchange repulsion. The pressure tensor, which is calculated in QDO\_MD from the atomic virial expression is currently being converted to a virial form based on heavy atom centres. Following the code convention, all interactions are splined.

APIMD-QDO integration is done in the canonical ensemble using a velocity Verlet propagator with RESPA and due to separation of the nuclear and QDO degrees of freedom this implementation requires separate thermostats for the Drude and atomic degrees of freedom. The separation is controlled by the adiabaticity parameter  $\gamma$ , with QDO degrees of freedom kept at elevated temperature. In order to remove large vacuum energy of the Drude subsystem, low variance harmonic staging virial estimator [25] acting on QDO sites only has been implemented to sample the instantaneous energy. Since APIMD-QDO is incompatible with certain molecular systems, e.g., in the current implementation the QDO molecules cannot simultaneously have the holonomic constraints, the program performs a set of checks before starting the simulation and logs the error if the conditions are violated.

APIMD-QDO can handle mixed systems, where only a subsystem contains QDO with the rest treated classically. Since in the APIMD-QDO algorithm all ingredients for the classical Drude oscillator are included, QDO\_MD could also simulate the classical polarizable molecules. These, however, cannot be mixed with QDOs.

## 6. QDO-water: an electronically-coarse grained model of water

The first application of QDOs to complex systems was water [23, 19]. Water was chosen due to its fundamental importance for life. Its properties have been studied for decades, yet the essential physics underlying many of its live-giving anomalies remains unresolved [55].

To construct a non-dissociative water model out of QDOs, one needs three elements: a rigid molecular frame with embedded point charges to replicate the lowest order electrostatic moments, a QDO to replicate electronic responses and a short range, pairwise repulsion potential. These elements are shown in Fig. 5 with their respective parameters given in Table 1.

In more detail, the frame is fixed in the experimental molecular geometry, with charges and distances chosen to give an exact dipole moment (1.85 D) and a best fit to the quadrupole moment. The parameters of the QDO

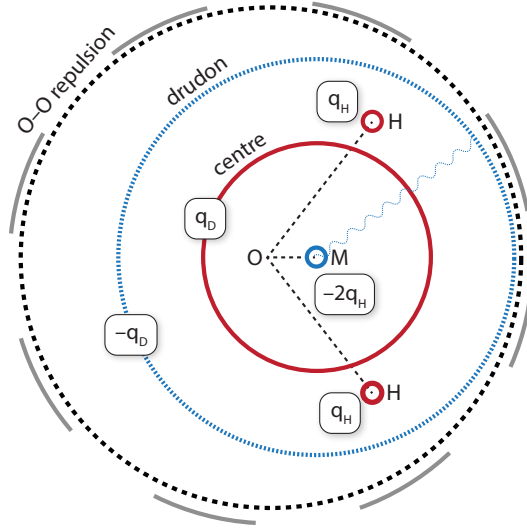


Figure 5: Schematic of QOD-water.

Parameter	Value	Parameter	Value
<b>Molecular geometry</b>		<b>Coulomb damping</b>	
$R_{OH}$	$0.9572 \text{ \AA}$	$\sigma_D = \sigma_H = \sigma_M$	$0.1 a_0$
$\angle HOH$	$104.52^\circ$	$\sigma_C$	$1.2 a_0$
<b>Ground state electrostatics</b>		<b>Short range repulsion</b>	
$q_H$	$0.605 e $	$\kappa_1$	$613.3 E_h$
$R_{OM}$	$0.2667 \text{ \AA}$	$\lambda_1$	$2.3244 a_0^{-1}$
<b>Quantum Drude Oscillator</b>		$\kappa_2$	$10.5693 E_h$
$m_D$	$0.3656 m_e$	$\lambda_2$	$1.5145 a_0^{-1}$
$\omega_D$	$0.6287 E_h/\hbar$		
$q_D$	$1.1973 e $		

Table 1: The free parameters of QDO-water.  $E_h \approx 27.211\text{eV}$  is the Hartree energy,  $a_0 \approx 0.5292\text{\AA}$  is the Bohr radius and  $e \approx 1.60 \times 10^{19} \text{ C}$  is the electron charge

are fit using the relations in equation (13) to the dipole and quadrupole polarisabilities and the  $C_6$  induced-dipole–induced-dipole dispersion coefficient. The repulsive potential is fit by calculating the interaction energy between two molecules using ab initio and the repulsion-free model and fitting the difference to a double exponential  $\kappa_1 e^{-\lambda_1 r} + \kappa_2 e^{-\lambda_2 r}$  [23, 19]. The Coulomb interaction between charges is regularised by replacing each point charge  $X$  by a Gaussian distribution of width  $\sigma_X$ .

Since QDO-water is parameterised from the properties of a single molecule and the dimer, condensed phase properties are a prediction rather than a fitting target. The model was studied in the following environments: high pressure ice (ice II) [19], liquid water [19], steam [19], the liquid-vapour interface [21] and supercritical water [20]. The agreement with experiment was good, with densities within few percent of experiment. The model predicts the temperature of maximum density of 5.5(2)°C (compared to the experimental value of 3.98°C [56]) and the critical point of {649(2)K, 0.317(5)g/cm<sup>3</sup>} (compared to the experimental value of {647.096K, 0.322g/cm<sup>3</sup>} [56]). It also accurately tracks the dielectric constant, enthalpy of vaporisation and surface tension between 300 K and 600 K [19].

QDO water also provided insights into the local structure at the liquid-vapour interface [21] and in supercritical water [20]. At the liquid-vapour interface the orientation of the water molecules is influenced by an intrinsic asymmetry in the way water molecules hydrogen bond. When losing a hydrogen bond, molecules prefer to lose it on the side of the oxygen (an acceptor bond) rather than on the side of the hydrogen (a donor bond) [21]. This leads to a surface with more oxygen than hydrogen atoms, which is negatively charged.

In supercritical water [20], the dipole moment was discovered to be a reliable fingerprint of the liquid-gas transition [20]. The phase diagram locus where the heat capacity is maximum coincides with a cusp in the dipole moment as a function of density. This cusp separates liquid-like from gas-like scaling, tracking the Widom line. This conclusion is general to any polar fluid, showing the importance of polarisation in characterising highly heterogeneous materials.

## 7. Conclusion

This paper summarises our recent progress in significantly enhancing the transferability of force fields describing complex systems of insulators by

coarse graining the electrons of a molecular moiety to a single quantum harmonic oscillator, known as a Quantum Drude Oscillator. This technique generates, naturally and to all orders, many-body forces such as dispersion, polarisation and mixed interactions beyond the dipole limit. These interactions are important in modelling heterogeneous environments such as those occurring in biological systems, where the symmetry of interactions depends strongly on environment. To demonstrate the application of the model, we highlight the successful construction of a transferable model of a water molecule. The model is parametrised using only the properties of a single molecule and those of a dimer yet has excellent predictive power across the phase diagram, from high pressure ice to supercritical water. To encourage the adoption of the method, we present its first implementation in the general purpose molecular dynamics software QDO\_MD.

## 8. Acknowledgements

This work was supported by the NPL Strategic Research programme. FSC acknowledges the Scottish Doctoral Training Centre in Condensed Matter Physics, NPL and EPSRC for funding under an Industrial CASE studentship. We acknowledge use of Hartree Centre resources in this work, including those from the Intel<sup>®</sup> Parallel Computing Centre.

## Appendix A. Coefficients

For a quantum Drude oscillator of mass  $m$ , charge  $q$  and frequency  $\omega$ , the coefficients defined in the text have the following values,

$$\begin{aligned}\alpha_P(\beta) &= \frac{m\omega}{2\hbar \sinh(f)}, \\ \lambda_P(\beta) &= \frac{2m\omega \tanh(f/2)}{\hbar}, \\ f &= \frac{\beta\hbar\omega}{P}\end{aligned}\tag{A.1}$$

The staging transformation uses the following coefficients:

$$\begin{aligned}
\vec{u}_1 &= \vec{x}_1, \\
\vec{u}_i &= \vec{x}_i - \vec{x}_i^*, \\
\vec{x}_i^* &= \frac{\sinh(\tau\hbar\omega)}{\sinh[i\tau\hbar\omega]}\vec{x}_1 + \frac{\sinh((i-1)\tau\hbar\omega)}{\sinh(i\tau\hbar\omega)}\vec{x}_{i+1}, \\
\sigma_1^2 &= \frac{\hbar}{2m\omega \tanh(\beta\hbar\omega/2)}, \\
\sigma_i^2 &= \frac{\hbar \sinh[(i-1)\tau\hbar\omega] \sinh(\tau\hbar\omega)}{m\omega \sinh[i\tau\hbar\omega]}.
\end{aligned} \tag{A.2}$$

## References

- [1] W. Cochran, Lattice dynamics of alkali halides, *Philosophical Magazine* 4 (45) (1959) 1082–1086. doi:10.1080/14786435908238288.
- [2] M. Sangster, M. Dixon, Interionic potentials in alkali halides and their use in simulations of the molten salts, *Advances in Physics* 25 (3) (1976) 247–342. doi:10.1080/00018737600101392.
- [3] J. Barker, Many-body interactions in rare gases, *Molecular Physics* 57 (4) (1986) 755–760. doi:10.1080/00268978600100541.
- [4] J. A. Barker, Many-body interactions in rare gases: Krypton and xenon, *Phys. Rev. Lett.* 57 (2) (1986) 230–233. doi:10.1103/physrevlett.57.230.
- [5] J. O. Hirschfelder, C. F. Curtiss, R. B. Bird, *The Molecular Theory of Gases and Liquids*, Wiley-Interscience, 1964.
- [6] J. R. Schames, R. H. Henchman, J. S. Siegel, C. A. Sotriffer, H. Ni, J. A. McCammon, Discovery of a novel binding trench in HIV integrase, *J. Med. Chem.* 47 (8) (2004) 1879–1881. doi:10.1021/jm0341913.
- [7] J. D. Durrant, J. A. McCammon, Molecular dynamics simulations and drug discovery, *BMC Biol* 9 (1) (2011) 71. doi:10.1186/1741-7007-9-71.

- [8] D. Frank, R. Dennard, E. Nowak, P. Solomon, Y. Taur, H.-S. P. Wong, Device scaling limits of si MOSFETs and their application dependencies, *Proceedings of the IEEE* 89 (3) (2001) 259–288. doi:10.1109/5.915374.
- [9] R. Dennard, F. Gaensslen, H.-N. Yu, V. Rideout, E. Bassous, A. Leblanc, Design of ion-implanted MOSFET's with very small physical dimensions, *Proceedings of the IEEE* 87 (4) (1999) 668–678. doi:10.1109/jproc.1999.752522.
- [10] J. C. Phillips, R. Braun, W. Wang, J. Gumbart, E. Tajkhorshid, E. Villa, C. Chipot, R. D. Skeel, L. Kalé, K. Schulten, Scalable molecular dynamics with NAMD, *J. Comput. Chem.* 26 (16) (2005) 1781–1802. doi:10.1002/jcc.20289.
- [11] M. E. Tuckerman, D. Yarne, S. O. Samuelson, A. L. Hughes, G. J. Martyna, Exploiting multiple levels of parallelism in molecular dynamics based calculations via modern techniques and software paradigms on distributed memory computers, *Comp. Phys. Comm.* 128 (2000) 333–376. doi:10.1016/S0010-4655(00)00077-1.
- [12] E. Bohm, A. Bhatele, L. V. Kale, M. E. Tuckerman, S. Kumar, J. A. Gunnels, G. J. Martyna, Fine-grained parallelization of the Car-Parrinello ab initio molecular dynamics method on the IBM Blue Gene/L supercomputer, *IBM Journal of Research and Development* 52 (1.2) (2008) 159–175. doi:10.1147/rd.521.0159.
- [13] R. V. Vadali, Y. Shi, S. Kumar, L. V. Kale, M. E. Tuckerman, G. J. Martyna, Scalable fine-grained parallelization of plane-wave-based ab initio molecular dynamics for large supercomputers, *J. Comput. Chem.* 25 (16) (2004) 2006–2022. doi:10.1002/jcc.20113.
- [14] D. C. Rapaport, *The Art of Molecular Dynamics Simulation*, Cambridge University Press, 2004.
- [15] D. J. Hazuda, N. J. Anthony, R. P. Gomez, S. M. Jolly, J. S. Wai, L. Zhuang, T. E. Fisher, M. Embrey, J. P. Guare, M. S. Egbertson, J. P. Vacca, J. R. Huff, P. J. Felock, M. V. Witmer, K. A. Stillmock, R. Danovich, J. Grobler, M. D. Miller, A. S. Espeseth, L. Jin, I.-W. Chen, J. H. Lin, K. Kassahun, J. D. Ellis, B. K. Wong, W. Xu, P. G.

- Pearson, W. A. Schleif, R. Cortese, E. Emini, V. Summa, M. K. Holloway, S. D. Young, J. M. Coffin, A naphthyridine carboxamide provides evidence for discordant resistance between mechanistically identical inhibitors of hiv-1 integrase, *Proc. Natl Acad. Sci. USA* 101 (31) (2004) 11233–11238. doi:10.1073/pnas.0402357101.
- [16] M. N. Offman, M. Krol, I. Silman, J. L. Sussman, A. H. Futerman, Molecular basis of reduced glucosylceramidase activity in the most common gaucher disease mutant, n370s, *Journal of Biological Chemistry* 285 (53) (2010) 42105–42114. doi:10.1074/jbc.m110.172098.
- [17] R. R. Wei, H. Hughes, S. Boucher, J. J. Bird, N. Guziewicz, S. M. V. Patten, H. Qiu, C. Q. Pan, T. Edmunds, X-ray and biochemical analysis of N370S mutant human acid  $\alpha$ -glucosidase, *Journal of Biological Chemistry* 286 (1) (2010) 299–308. doi:10.1074/jbc.m110.150433.
- [18] Y. Wang, T. Zhao, D. Wei, E. Strandberg, A. S. Ulrich, J. P. Ulmschneider, How reliable are molecular dynamics simulations of membrane active antimicrobial peptides?, *Biochimica et Biophysica Acta (BBA) - Biomembranes* 1838 (9) (2014) 2280–2288. doi:10.1016/j.bbamem.2014.04.009.
- [19] V. P. Sokhan, A. P. Jones, F. S. Cipcigan, J. Crain, G. J. Martyna, Signature properties of water: Their molecular electronic origins, *Proc. Natl Acad. Sci. USA* 112 (20) (2015) 6341–6346. doi:10.1073/pnas.1418982112.
- [20] V. P. Sokhan, A. Jones, F. S. Cipcigan, J. Crain, G. J. Martyna, Molecular-scale remnants of the liquid-gas transition in supercritical polar fluids, *Phys. Rev. Lett.* 115 (11). doi:10.1103/physrevlett.115.117801.
- [21] F. S. Cipcigan, V. P. Sokhan, A. P. Jones, J. Crain, G. J. Martyna, Hydrogen bonding and molecular orientation at the liquid–vapour interface of water, *Phys. Chem. Chem. Phys.* 17 (14) (2015) 8660–8669. doi:10.1039/c4cp05506c.
- [22] A. Jones, J. Crain, F. Cipcigan, V. Sokhan, M. Modani, G. Martyna, Electronically coarse-grained molecular dynamics using quantum Drude

- oscillators, *Mol. Phys.* 111 (22-23) (2013) 3465–3477. doi:10.1080/00268976.2013.843032.
- [23] A. Jones, F. Cipcigan, V. P. Sokhan, J. Crain, G. J. Martyna, Electronically coarse-grained model for water, *Phys. Rev. Lett.* 110 (22). doi:10.1103/physrevlett.110.227801.
- [24] T. W. Whitfield, G. J. Martyna, A unified formalism for many-body polarization and dispersion: The quantum Drude model applied to fluid xenon, *Chem. Phys. Lett.* 424 (4-6) (2006) 409–413. doi:10.1016/j.cpllett.2006.04.035.
- [25] T. W. Whitfield, G. J. Martyna, Low variance energy estimators for systems of quantum Drude oscillators: Treating harmonic path integrals with large separations of time scales, *J. Chem. Phys.* 126 (2007) 074104. doi:10.1063/1.2424708.
- [26] A. P. Jones, J. Crain, V. P. Sokhan, T. W. Whitfield, G. J. Martyna, Quantum drude oscillator model of atoms and molecules: Many-body polarization and dispersion interactions for atomistic simulation, *Phys. Rev. B* 87 (14). doi:10.1103/physrevb.87.144103.
- [27] M. Chaplin, Water structure and science, [www1.lsbu.ac.uk/water/](http://www1.lsbu.ac.uk/water/), (Accessed on 15 March 2016).
- [28] N. Chentanez, M. Müller, Real-time eulerian water simulation using a restricted tall cell grid, *ACM Trans. Graph.* 30 (2011) 82:1–82:10. doi:10.1145/2010324.1964977.
- [29] A. J. Stone, A. J. Misquitta, Atom–atom potentials from ab initio calculations, *International Reviews in Physical Chemistry* 26 (1) (2007) 193–222. doi:10.1080/01442350601081931.
- [30] D. D. Kemp, M. S. Gordon, An interpretation of the enhancement of the water dipole moment due to the presence of other water molecules, *J. Phys. Chem. A* 112 (22) (2008) 4885–4894. doi:10.1021/jp801921f.
- [31] G. G. Simeoni, T. Bryk, F. A. Gorelli, M. Krisch, G. Ruocco, M. Santoro, T. Scopigno, The widom line as the crossover between liquid-like and gas-like behaviour in supercritical fluids, *Nat Phys* 6 (7) (2010) 503–507. doi:10.1038/nphys1683.

- [32] B. Widom, Surface tension of fluids, in: C. Domb, M. S. Green (Eds.), *Phase Transitions and Critical Phenomena*, Academic Press, 1972, pp. 79–99.
- [33] I.-C. Lin, A. P. Seitsonen, I. Tavernelli, U. Rothlisberger, Structure and dynamics of liquid water from ab initio molecular dynamics—comparison of BLYP, PBE, and revPBE density functionals with and without van der waals corrections, *J. Chem. Theory Comput.* 8 (10) (2012) 3902–3910. doi:10.1021/ct3001848.
- [34] A. Tkatchenko, R. A. DiStasio, R. Car, M. Scheffler, Accurate and efficient method for many-body van der waals interactions, *Phys. Rev. Lett.* 108 (23). doi:10.1103/physrevlett.108.236402.
- [35] F. N. Keutsch, J. D. Cruzan, R. J. Saykally, The water trimer, *Chem. Rev.* 103 (7) (2003) 2533–2578. doi:10.1021/cr980125a.
- [36] M. E. Johnson, T. Head-Gordon, A. A. Louis, Representability problems for coarse-grained water potentials, *J. Chem. Phys.* 126 (14) (2007) 144509. doi:10.1063/1.2715953.
- [37] A. Chaimovich, M. S. Shell, Anomalous waterlike behavior in spherically-symmetric water models optimized with the relative entropy, *Phys. Chem. Chem. Phys.* 11 (12) (2009) 1901. doi:10.1039/b818512c.
- [38] C. Vega, J. L. F. Abascal, Relation between the melting temperature and the temperature of maximum density for the most common models of water, *J. Chem. Phys.* 123 (14) (2005) 144504. doi:10.1063/1.2056539.
- [39] J. O. Hirschfelder, C. F. Curtiss, R. B. Bird, *The Molecular Theory of Gases and Liquids*, Wiley-Interscience, 1964.
- [40] P. R. Fontana, Theory of long-range interatomic forces. i. dispersion energies between unexcited atoms, *Phys. Rev.* 123 (5) (1961) 1865–1870. doi:10.1103/physrev.123.1865.
- [41] M. Parrinello, A. Rahman, Study of an f center in molten KCl, *The Journal of Chemical Physics* 80 (2) (1984) 860. doi:10.1063/1.446740.

- [42] M. E. Tuckerman, B. J. Berne, G. J. Martyna, M. L. Klein, Efficient molecular dynamics and hybrid monte carlo algorithms for path integrals, *The Journal of Chemical Physics* 99 (4) (1993) 2796. doi: 10.1063/1.465188.
- [43] R. P. Feynman, *Statistical Mechanics: A Set Of Lectures* (Advanced Books Classics), Westview Press, 1998.
- [44] H. F. Trotter, On the product of semi-groups of operators, *Proceedings of the American Mathematical Society* 10 (4) (1959) 545–545. doi: 10.1090/s0002-9939-1959-0108732-6.
- [45] L. V. Kalé, K. Schulten, R. D. Skeel, G. Martyna, M. Tuckerman, J. C. Phillips, S. Kumar, G. Zheng, Biomolecular modeling using parallel supercomputers, in: *Chapman & Hall/CRC Computer & Information Science Series*, Chapman and Hall/CRC, 2005, pp. 34–1–34–43. doi:10.1201/9781420036275.ch34.
- [46] R. H. Swendsen, J.-S. Wang, Replica Monte Carlo simulation of spin-glasses, *Phys. Rev. Lett.* 57 (1986) 2607–2609. doi:10.1103/PhysRevLett.57.2607.
- [47] M. Tuckerman, B. J. Berne, G. J. Martyna, Reversible multiple time scale molecular dynamics, *J. Chem. Phys.* 97 (3) (1992) 1990–2001. doi: 10.1063/1.463137.
- [48] G. J. Martyna, M. L. Klein, M. Tuckerman, Nosé–Hoover chains: The canonical ensemble via continuous dynamics, *J. Chem. Phys.* 97 (4) (1992) 2635–2643. doi:10.1063/1.463940.
- [49] G. J. Martyna, D. J. Tobias, M. L. Klein, Constant pressure molecular dynamics algorithms, *J. Chem. Phys.* 101 (5) (1994) 4177–4189. doi: 10.1063/1.467468.
- [50] A. B. K. Collis, A performance analysis of two ab initio molecular dynamics simulation codes, MSc Report, The University of Edinburgh (2009).
- [51] M. Forum, MPI - a Message Passing Interface Standard V3.1. Ean 1114444410030, High Performance Computing Center, Stuttgart (HLRS), 2015, (Accessed on 15 March 2016).

- [52] U. Essmann, L. Perera, M. L. Berkowitz, T. Darden, H. Lee, L. G. Pedersen, A smooth particle mesh Ewald method, *J. Chem. Phys.* 103 (19) (1995) 8577–8593. doi:10.1063/1.470117.
- [53] G. J. Martyna, M. E. Tuckerman, A reciprocal space based method for treating long range interactions in ab initio and force-field-based calculations in clusters, *J. Chem. Phys.* 110 (6) (1999) 2810–2821. doi:10.1063/1.477923.
- [54] P. Mináry, M. E. Tuckerman, K. A. Pihakari, G. J. Martyna, A new reciprocal space based treatment of long range interactions on surfaces, *J. Chem. Phys.* 116 (13) (2002) 5351–5362. doi:10.1063/1.1453397.
- [55] C. A. Angell, Supercooled water: Two phases?, *Nature Materials* 13 (7) (2014) 673–675. doi:10.1038/nmat4022.
- [56] W. Wagner, A. Pruß, The IAPWS formulation 1995 for the thermodynamic properties of ordinary water substance for general and scientific use, *Journal of Physical and Chemical Reference Data* 31 (2) (1999) 387. doi:10.1063/1.1461829.